Ultrahigh-Temperature Metamorphism in the Palni Hills, South India: Insights from Feldspar Thermometry and Phase Equilibria

D. PRAKASH,[1]

Department of Geology, Banaras Hindu University, Varanasi-221005, India

M. ARIMA,

Geological Institute, Yokohama National University, 79-7 Tokiwadai, Hodogaya-ku, Yokohama 240-8501, Japan

AND A. MOHAN

Department of Geology, Banaras Hindu University, Varanasi-221005, India

Abstract

The Southern Indian shield is a classic terrain that may be regarded as a model for Precambrian crustal evolution. The Palni Hills represent a portion of the granulite-facies terrain of the Madurai block. Determination of ultrahigh temperature (UHT) in granulites requires re-integration of anti-perthite, perthite, and mesoperthite to yield original hypersolvus feldspar compositions, which then yield peak metamorphic temperatures by feldspar solvus geothermometry. Backscattered electron images were used to calculate modal proportions of host and exsolved lamellae in feldspars. These data were combined with quantitative point chemical analyses of both host and lamellae to obtain re-integrated feldspar compositions, providing consistent ultrahigh temperatures in excess of 900°C. The feldspar compositions coexisting during closure of intercrystalline Al-Si exchange were calculated by reversing the K-Na exchange through shifts of Ab and Or contents of both feldspars at constant An contents until the equilibrium tie-line and the common isotherm on the ternary feldspar solvus were found. Besides, UHT metamorphic conditions were also obtained using the convergence method in exchange thermometers, suggesting peak metamorphism conditions at > 900°C at 9 kbar for the Palni granulites. Prevalence of UHT conditions in the many parts of the world could be useful in deducing Proterozoic tectonometamorphic processes along the deep crust-mantle interface.

Introduction

ULTRAHIGH-TEMPERATURE metamorphism with a peak at 900–1100°C, 7–13 kbar implies extreme conditions of metamorphism for the granulite facies rocks of the lower continental crust (Harley, 1998a). Corona and symplectitic reaction textures in granulites have been used to deduce reaction histories and P-T paths of UHT terrains (Harley, 1989, 1998a). Ultrahigh temperature metamorphism has been increasingly reported in granulites using feldspar thermometry from several Precambrian regional terrains around the world (Hayob et al., 1989; Braun et al., 1996; Raase, 1998; Yoshimura et al., 2000; Hokada, 2001).

The Palni Hills and adjoining areas have attracted the attention of petrologists on account of

UHT granulites that serve as a window into the mid-lower continental crust. The study area, situated in the Palni Hills of the Madurai block, lies between the Palghat-Cauvery and the Achankovil shear zones (Fig. 1A). The Palni Hills form part of the Kodaikanal massif, one of the largest highland blocks of granulites in southern India (Fig. 1B). Charnockites, mafic granulites, metasediments, hornblende gnesises, and discrete bodies of granite comprise the principal lithologies of the Palni Hills.

Common mineral assemblages of constituent metapelites include garnet, cordierite, sapphirine, orthopyroxene, spinel, and sillimanite. The garnet-cordierite-sapphirine–bearing assemblages dominantly occur in the central part of the highland massif, whereas garnet-sillimanite–bearing assemblages prevail in the Ganguvarpatti-Andipatti-Usilampatti lowland massif. Marble and calc-silicate are carbonate lithologies that in addition locally contain

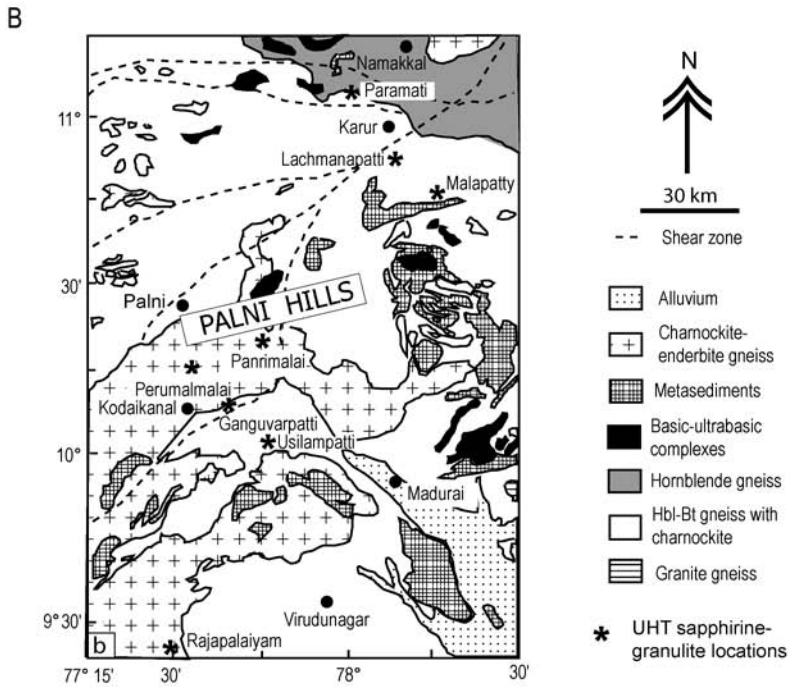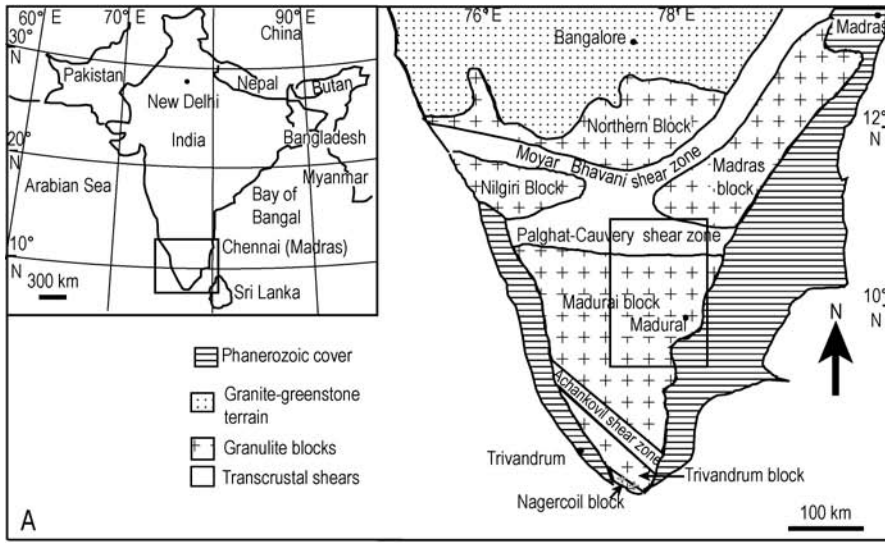[1]Corresponding author; email: dprakash_vns@rediffmail.com

FIG. 1. A. Gerneral geologic map of South India, showing different granulite blocks and major Proterozoic shear zones (modified from Harris et al., 1994). Inset shows an index map of India. B. Geological map of the Madurai block and part of the Palghat-Cauvery shear zone.

quartzites and ultramafics. Sapphirine-bearing granulites have been reported previously from a number of localities in the central and northern parts of the Madurai block. These sapphirine-bearing granulites revealed UHT metamorphism (see Fig. 1B) in several localities, e.g. Rajapalaiyam (Sriramguru et al., 2002; Tateishi et al., 2004), Perumalmalai (Mohan et al., 1996; Raith et al., 1997; Prakash and Arima, 2003), Ganguvarpatti (Sajeev et al., 2004; Tamashiro et al., 2004; Das et al., 2005; Mohan et al., 2005), Usilampatti (Prakash and Arima, 2003), Lachmanapatti (Tsunogae and Santosh, 2003), Malappatty (Tsunogae and Santosh, 2003), and Paramatti, in the Palghat-Cauvery zone (Koshimoto et al., 2004). Previous studies of UHT metamorphism of rocks of the Madurai block were inferred only from the sapphirine-granulites using phase equilibria and textural relationships. Exsolution textures of feldspars from granulite terrains potentially record information about UHT metamorphism, but have been little studied as yet. The results presented here suggest that the ternary feldspar solvus is an effective tool for estimating peak metamorphic condition. This paper aims at determining metamorphic peak conditions of the granulites using feldspar thermometry and retrieval calculations. We report for the first time the existence of UHT metamorphic conditions from other rock types of the Palni Hills besides the sapphirine-granulites mentioned above.

Textural Relations

Sapphirine-bearing granulites

Sapphirine-bearing granulites have been reported from the several localities from the Palni Hills and adjoining area (Fig. 1B). The granulites display granoblastic textures consisting of a mosaic of hypersthene–cordierite-sapphirine-spinel. In a few samples, one set of prominent foliation is defined by the parallel orientation of phlogopite, hypersthene, and sillimanite. Locally, two sets of foliation are present at oblique angles. Textural relations of sapphirine-bearing granulites from Usilampatti and Perumalmali have been extensively described by Prakash and Arima (2003). A typical feature of the Palni granulites is the preservation of feldspar exsolution textures.

Two types of feldspar assemblage can be distinguished: (I) antiperthite and alkali feldspar; and (II) mesoperthite. Generally, assemblage I predominates in the granulites of the Ganguvarpatti and Usilam-patti areas, but the feldspars of the Perumalmali area are regular mesoperthitic belonging to the type II assemblage (Figs. 2A and 2B). Regular and irregular exsolution textures (Figs. 3A and 3B), typical of mesoperthite, are interpreted as evidence for slow cooling from the thermal peak of regional metamorphism. Mesoperthite with fine K-feldspar lamellae (1.0–12 µm wide) is replaced by an oblique set of plagioclase lamellae (Figs. 3C and 3D). The average re-integrated compositions of mesoperthite domains for the sapphirine-bearing granulites cluster in the range of $Or_{30-46}Ab_{45-61}An_{6-11}$ (Table 1).

Garnet-orthopyroxene–bearing gneisses

Banded garnet-orthopyroxene–bearing gneisses are foliated with alternating layers of dark and light colored minerals. The quartzofeldspathic bands are rich in potash-feldspar, with minor quartz and garnet. Feldspar is the main constituent, which imparts a flesh color to the rock apart from the quartz, spinel, apatite, and magnetite, which are common accessories. Plagioclase is antiperthitic and unzoned. Patches of K-feldspar are elongated and parallel (Figs. 2C and 2D). Lamellae of the K-rich phase are generally 10–30 µm thick (Figs. 3E and 3F).

Garnet-sillimanite ± cordierite gneisses

The most abundant antiperthite texture is found in all garnet-cordierite gneisses. A crude foliation is defined by elongated hypersthene prisms and biotite flakes. Rods and lamellae of K-rich phase are generally ~50 µm thick (Figs. 3G and 3H). Antiperthites in garnet-cordierite gneisses display greater widths of K-feldspar lamellae.

Charnockites

The majority of these rocks are characterized by granoblastic textures with perthite and antiperthite (Figs. 2E and 2F). Equigranular texture and predominance of alkali-feldspars (perthite > plagioclase) are conspicuous features of the charnockites. They are composed of crystalline aggregates of quartz and alkali-feldspar, with subordinate oligoclase, hypersthene, and iron oxides.

Feldspar Geothermometery

Evaluation of the reliability of conventional exchange thermometry shows that even core compositions of grains in contact with exchangeable neighbors may be reset, and may not record peak temperatures of metamorphism (Pattison and Begin,
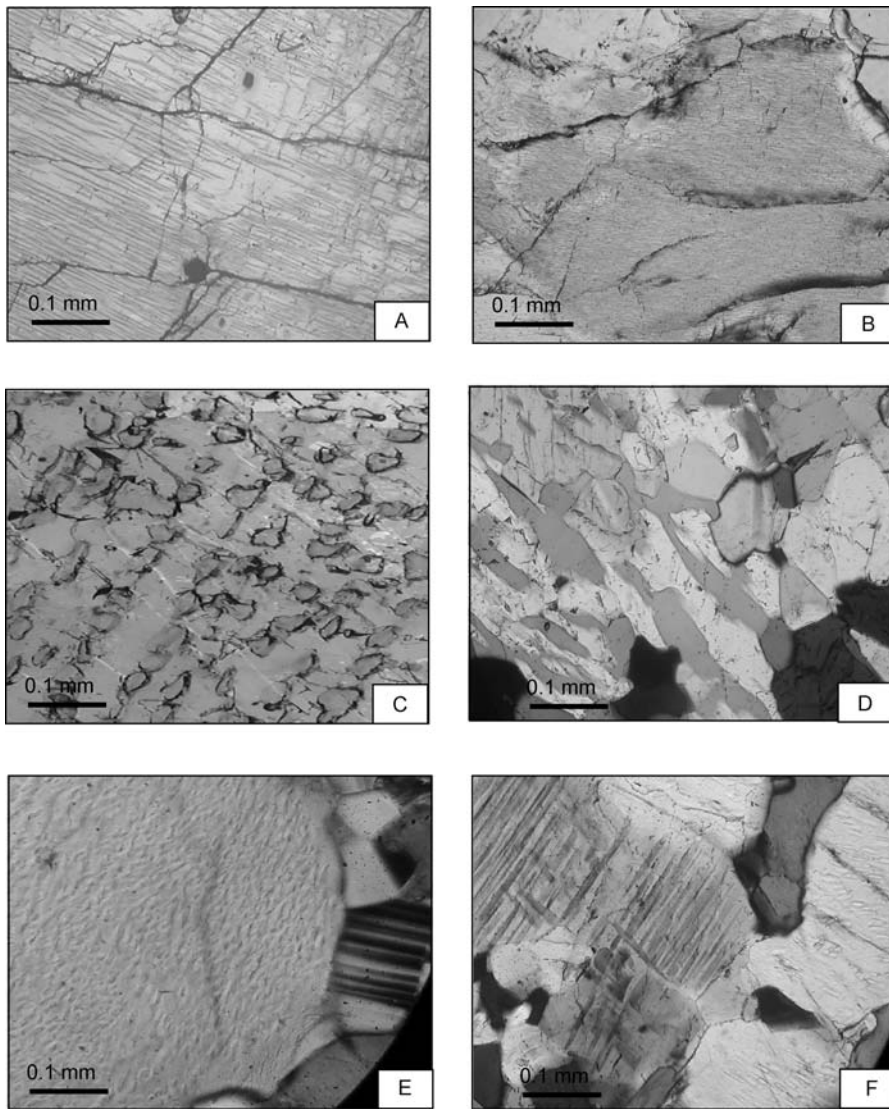
FIG. 2. Photomicrographs showing textures of exsolved feldspar in granulites from the Palni Hills. A and B. Photomicrographs showing mesoperthites in sapphirine-bearing granulites. C and D. Antiperthitic plagioclase containing exsolved rods of K-feldspar in garnet-orthopyroxene–bearing gneisses. Antiperthitic plagioclase grains containing exsolved patches of K-feldspar are elongated and parallel. E. Perthitic alkali feldspar with plagioclase in charnockites. F. Antiperthite with alkali feldspar in charnockites.

1994). The blocking effect in the granulites as observed in the empirically calibrated exchange thermometry indicates significant departures from the thermal peak of metamorphism. Such conventional thermometry is fraught with the problem that they record invariably lower temperature conditions than that attained during peak granulite metamor-

phism. For a meaningful interpretation of temperatures obtained from these thermometers, it is essential to consider the effect of closure temperature and also the extent of re-equilibration during cooling. Frost and Chacko (1989) suggested re-integration of exsolved lamellae to overcome this problem. Re-integration of the original composition of
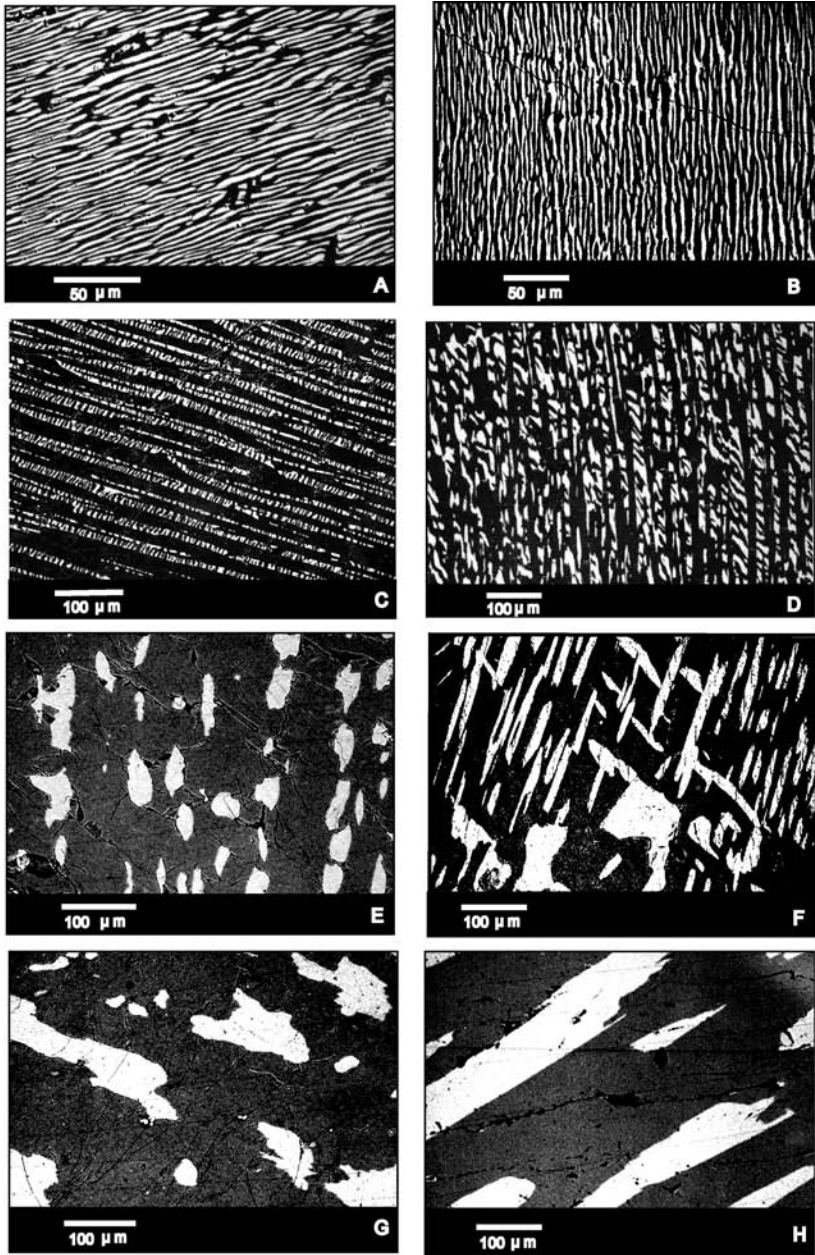
FIG. 3. A and B. Backscattered electron images of a typical mesoperthite, showing the regular and continuous nature of exsolved plagioclase. C and D. Backscattered electron images of a mesoperthite with fine K-feldspar lamellae (1.0–12 μm wide) replaced by an oblique set of plagioclase lamellae. E and F. Backscattered electron images of antiperthite, with lamellae of K-rich phase, generally 10–30 μm in thickness. G and H. Backscattered electron images of antiperthite, with rods and lamellae of K-rich phase generally ~50 μm in thickness.

TABLE 1. Re-integrated Average Compositions of Mesoperthite for Sapphirine-Bearing Granulites

Rock type:							Sapphirine-bearing granulites				
Sample no.:	51	51	51	42	42	42	737	737	737	40	40	40
SiO_2	64.81	64.23	63.11	64.824	64.59	64.32	62.88	64.668	63.135	64.182	64.39	64.722
TiO_2	0.00	0.00	0.00	0.45	0.00	0.00	0.17	0.00	0.16	0.00	0.00	0.00
Al_2O_3	20.38	20.63	21.02	19.24	21.96	19.73	20.19	20.86	20.68	20.97	20.68	20.20
Cr_2O_3	0.00	0.00	0.00	0.00	0.00	0.00	0.00	0.00	0.00	0.00	0.00	0.00
FeO	0.00	0.00	0.00	0.00	0.36	0.00	0.00	0.00	0.22	0.00	0.00	0.37
MnO	0.02	0.21	0.00	0.00	0.00	0.00	0.00	0.00	0.00	0.00	0.00	0.00
MgO	0.00	0.00	0.00	0.00	0.00	0.00	0.00	0.00	0.00	0.00	0.00	0.00
CaO	1.69	1.32	2.10	1.89	1.38	1.78	2.11	2.01	2.56	1.98	2.00	2.14
Na_2O	6.39	6.25	7.00	5.28	4.99	5.89	7.26	7.23	7.10	5.71	6.14	7.12
K_2O	6.31	6.68	6.64	8.13	6.42	8.12	6.89	5.21	6.11	6.73	6.11	5.18
Total	99.60	99.32	99.87	99.81	99.70	99.89	99.50	99.98	99.97	99.58	99.32	99.73
O	8.00	8.00	8.00	8.00	8.00	8.00	8.00	8.00	8.00	8.00	8.00	8.00
Si	2.918	2.906	2.858	2.935	2.891	2.917	2.868	2.895	2.857	2.894	2.905	2.909
Ti	0.000	0.000	0.000	0.015	0.000	0.000	0.006	0.000	0.005	0.000	0.000	0.000
Al	1.081	1.100	1.122	1.027	1.159	1.057	1.086	1.101	1.103	1.115	1.100	1.070
Cr	0.000	0.000	0.000	0.000	0.000	0.000	0.000	0.000	0.000	0.000	0.000	0.000
Fe	0.000	0.000	0.000	0.000	0.000	0.000	0.000	0.000	0.008	0.000	0.000	0.014
Mn	0.001	0.008	0.000	0.000	0.013	0.000	0.000	0.000	0.000	0.000	0.000	0.000
Mg	0.000	0.000	0.000	0.000	0.000	0.000	0.000	0.000	0.000	0.000	0.000	0.000
Ca	0.082	0.064	0.102	0.092	0.066	0.086	0.103	0.096	0.124	0.096	0.097	0.103
Na	0.558	0.548	0.615	0.464	0.433	0.518	0.642	0.628	0.623	0.500	0.537	0.621
K	0.362	0.386	0.384	0.470	0.367	0.470	0.401	0.298	0.353	0.387	0.352	0.297
An	0.081	0.064	0.093	0.089	0.076	0.081	0.090	0.094	0.113	0.097	0.098	0.101
Ab	0.557	0.549	0.559	0.452	0.500	0.482	0.560	0.614	0.566	0.508	0.545	0.608
Or	0.362	0.386	0.349	0.458	0.423	0.437	0.350	0.291	0.321	0.394	0.357	0.291

antiperthite, mesoperthite, and perthite was done by image analysis. Backscattered electron images were used to calculate the modal proportion of host and lamellae feldspar in the different exsolutions. These data were combined with quantitative analysis of individual spots on the host and the lamellae to obtain re-integrated feldspar compositions.

The re-integrated bulk compositions of the antiperthites coexisting with unexsolved alkali feldspars and perthites coexisting with unexsolved plagioclase are listed in Table 2. The re-integration procedure was applied to core compositions of the feldspars because it minimizes the possibilities of resetting during retrogression and cooling. The recalculated compositions obtained by reversing the intercrystalline K-Na exchange (Kroll et al., 1993) and subsequently two-feldspar temperatures calculated with Margules parameters (Fuhrman and Lindsley, 1988; Lindsley and Nekvasil, 1989; Elkins and Grove, 1990) are given in Table 2. Recalculation was done by the computer programs F-THERM, L-THERM, and E-THERM (Kroll et al., 1993). Al-Si exchange between plagioclase (antiperthite) and alkali feldspar ceases at relatively high temperatures, whereas alkali exchange continues during cooling, from which a minimum temperature of feldspar equilibration can be obtained. The composition of the feldspars at the time of closure of intercrystalline Al-Si exchange is obtained through shifts of Ab and Or contents of both feldspars at constant An contents until the equilibrium tie-line and the common isotherm on the ternary feldspar solvus are found (cf. Raase, 1998 and the references therein). The calculated temperatures should be close to those of the peak metamorphism, because Al-Si exchange is very slow, even at high temperature (Grove et al., 1984; Yund, 1986; Liu and Yund, 1992; Raase, 1998).

Sapphirine-bearing granulites

Core composition of the feldspars from the sapphirine-bearing granulites gave a temperature of 968°C using the Margules parameters of Fuhrman and Lindsley (1989). Temperature estimates obtained from Fuhrman and Lindsley (1989) and Lindsley and Nekvasil (1989) yield broadly similar results, but are relatively higher (50–60°C) compare to the model of Elkins and Grove (1990) (see Table 2). Variations in temperature estimates are consequences of differences in the activity-composition relations and the input thermodynamic data used in these models. By reversing K-Na exchange, the Or

component of the plagioclase changes slightly, whereas the alkali feldspar becomes much more Ab rich. Such variation in composition could be related to the low ratio of alkali feldspar to plagioclase in the sapphirine-bearing granulites. Analyzed and calculated compositions of sapphirine-granulites are plotted in the An-Ab-Or diagram (Fig. 4). The ultrahigh temperatures obtained for the sapphirine-bearing granulites are compatible with temperatures (900–1000°C) reported from the Palni Hills (Raith et al., 1997; Prakash and Arima, 2003) as well as those derived from the garnet-orthopyroxene Al-solubility based thermobarometry corrected for late Fe-Mg exchange in the present study.

A few samples of sapphirine-bearing granulites contain mesoperthite, which do not coexist with plagioclase. The re-integrated composition of mesoperthite suggests a temperature range of 900–1000°C (using isotherms calculated after Fuhrman and Lindsley, 1988). These temperature values must be taken as minimum because the composition of mesoperthite was obtained by integrating results of electron-microprobe analyses (Fig. 5).

Garnet-orthopyroxene bearing gneisses

The calculated temperatures with the Margules parameters of Fuhrman and Lindsley (1989) for garnet-orthopyroxene bearing gneisses are 930–945°C (Table 2). Temperatures calculated using the Margules parameters of Lindsley and Nekvasil (1989) provide 45–50°C lower T estimates. Similarly, the Elkins and Grove (1990) model yields comparatively higher T values (~30–35°C). The analyzed and calculated compositions of garnet-orthopyroxene–bearing gneisses were plotted in the An-Ab-Or diagram (Fig. 4). Analyzed plagioclase and alkali feldspar do not match the calculated tie lines, suggesting that the plagioclase lost most of its Or content. By reversing the K-Na exchange with fixed An content for both feldspars, the plagioclase becomes more Or rich, whereas alkali feldspar becomes more Ab rich. These observations reflect the effect of retrograde intercrystalline K-Na exchange between plagioclase and alkali feldspar.

Garnet-sillimanite ± cordierite gneisses

Two-feldspar temperatures of 939 and 956°C were computed with antiperthite and alkali feldspar for fixed An contents of both feldspar (Kroll et al., 1993), using the Margules parameters of Fuhrman and Lindsley (1998) (Table 2). As shown in Figure 4, the analyzed plagioclase and alkali-feldspar

TABLE 2 . Compositions (analyzed and calculated) and Temperatures for Feldspar Pairs from Granulites of the Palni Hills, South India[1]

Sample no.	Feldspar	Composition			C(FL)			C(LN)			C(EG)			T(FL), °C	T(LN), °C	T(EG), °C
		Ab	Or	An	Ab	Or	An	Ab	Or	An	Ab	Or	An			
					Sapphirine–bearing granulites											
S13	Antiperthite(Pl)	57.6	19.4	23.0	56.4	20.6	23.0	56.8	20.2	23.0	56.9	20.1	23.0	968	979	1029
	Alkalifeldspar	29.8	62.4	7.8	35.5	56.7	7.8	37.8	54.4	7.8	39.7	52.5	7.8			
S27	Antiperthite(Pl)	58.1	20.2	21.7	57.0	21.3	21.7	57.9	20.4	21.7	57.2	21.1	21.7	968	973	1028
	alkalifeldspar	27.2	65.0	7.8	36.85	5.4	7.8	39.2	53.0	7.8	40.6	51.6	7.8			
					Garnet-orthopyroxene bearing gneisses											
D40	Antiperthite(Pl)	62.1	29.1	8.8	54.6	36.6	8.8	52.4	38.8	8.8	55.3	35.9	8.8	930	884	960
	Alkali Feldspar	41.8	52.2	6.0	46.5	47.5	6.0	43.8	50.2	6.0	48.1	45.9	6.0			
D42	Antiperthite(Pl)	61.5	28.2	10.3	56.6	33.1	10.3	51.9	37.8	10.3	57.3	32.4	10.3	945	900	978
	Alkali Feldspar	39.9	53.6	6.5	46.7	46.8	6.5	42.1	51.4	6.5	48.6	44.9	6.5			
					Garnet-sillimanite±cordierite gneisses											
N22	Antiperthite(Pl)	61.2	28.3	10.5	59.8	29.7	10.5	46.4	43.1	10.5	51.7	37.8	10.5	939	858	965
	Alkalifeldspar	27.8	66.1	6.1	47.8	46.1	6.1	36.2	57.7	6.1	42.3	51.6	6.1			
N35	Antiperthite(Pl)	63.0	20.1	16.9	59.2	23.9	16.9	61.5	21.6	16.9	56.9	26.2	16.9	956	938	1011
	Alkalifeldspar	26.7	66.4	6.9	40.5	52.6	6.9	42.7	50.4	6.9	41.6	51.5	6.9			
					Charnockites											
C10	Perthite	26.6	67.3	6.1	33.4	60.5	6.1	36.6	57.3	6.1	36.8	57.1	6.1	924	916	989
	Plagioclase	70.1	5.7	24.2	60.1	15.7	24.2	61.8	14.0	24.2	58.7	17.1	24.2			
C12	Perthite	27.1	65.7	7.2	33.1	59.7	7.2	38.5	54.3	7.2	56.5	18.4	25.1	955	940	1021
	Plagioclase	72.3	2.6	25.1	56.5	18.4	25.1	60.8	14.1	25.1	37.3	55.5	7.2			

[1]Calculated compositions (C) and temperatures (T) obtained by reversing the K-Na exchange according to Kroll et al. (1993), with the fixed An content of both feldspars . T(FL), T(LN), and T(EG) temperatures calculated with the margules parameters of Fuhrman and Lindsley (1988), Lindsley and Nekvasil (1989), and Elkins and Grove (1990) respectively at 9Kbar. Re-integrated compositions of antiperthite and perthite obtained by image analysis.
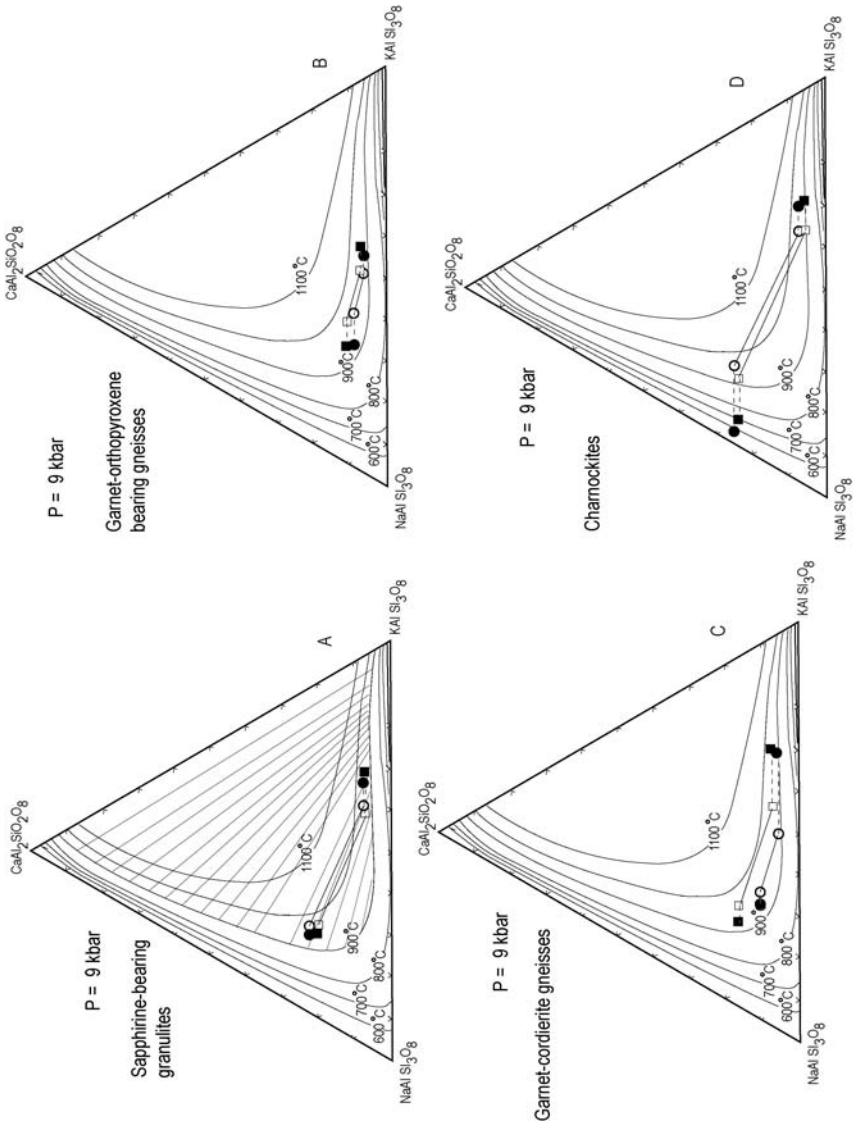
FIG. 4. A, B, and C show ternary plots of re-integrated feldspar compositions for analyzed (closed symbols) and calculated compositions (open symbols) of recrystallized antiperthite (plagioclase) alkali feldspar pairs in sapphirine-bearing granulites, garnet-orthopyroxene–bearing gneisses, and garnet-cordierite gneisses, respectively. Isotherms are according to Fuhrman and Lindsley (1988). The tie-lines for 900°C are also shown using Fuhrman and Lindsley (1988) in Figure 4A. D. Analyzed and calculated compositions of recrystallized perthite plagioclase pairs in charnockites.
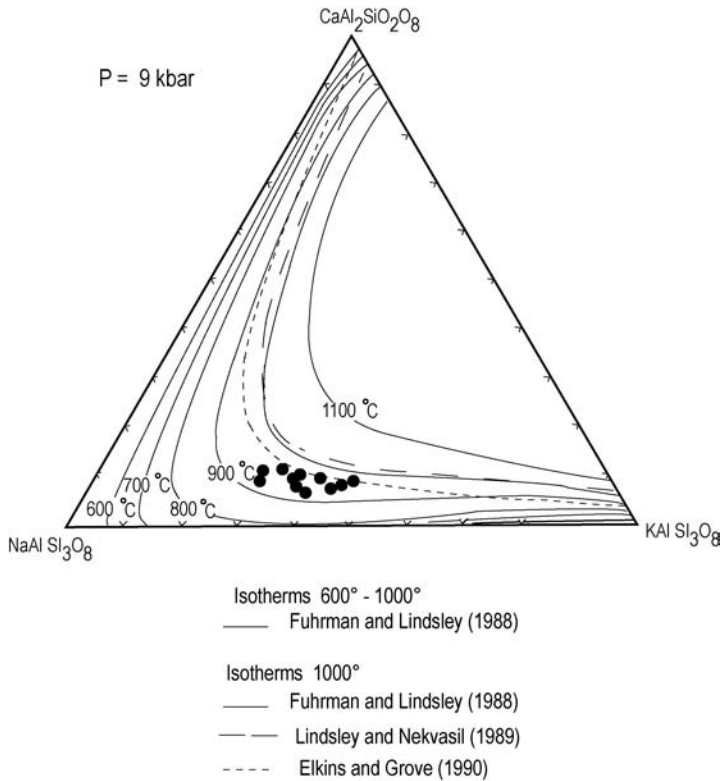
FIG. 5. Ternary feldspar diagram showing the location of the 600–1100°C solvi at 9 kbar and the composition of mesoperthites in sapphirine-bearing granulite (solid circles).

compositions do not plot on the same isotherm. Calculated compositions of the alkali feldspars are richer in Ab than the analyzed composition. This deviation has resulted from retrograde K-Na exchange.

Charnockites

Grains of alkali feldspar in the charnockites consist of string perthite, whereas coexisting plagioclase laths do not show any exsolution (Fig. 2E). In other domains, antiperthite coexists with alkali feldspar (Fig. 2F). The analyzed compositions do not plot on the same isotherm, but the calculated compositions obtained by reversing the K-Na exchange according to Kroll et al. (1993) with the fixed An content of both feldspars do plot on the same isotherm (Fig. 4). By reversing the K-Na exchange, alkali feldspars (perthite) become much more albite rich, and plagioclase becomes much more orthoclase rich.

Garnet-Orthopyroxene Al-Solubility–Based Thermobarometry Corrected for Late Fe-Mg Exchange

It is well known that because of intensive resetting and non-simultaneous closure of equilibria in such rocks during slow cooling, the thermal peak conditions and P-T trajectories cannot be reliably assessed by conventional thermometric techniques. Development of convergence techniques proposed by Pattison and Begin (1994) and Fitzsimons and Harley (1994) and refined by Chacko et al. (1996) has definite advantages because it not only aids retrieval of peak P-T conditions from high-grade metamorphic rocks, it also enhances our ability to characterize the P-T paths followed by individual rocks. Recently Pattison et al. (2003) reported a method using more recent thermodynamic data and applied it to a large number of granulites worldwide. Their approach is based on Al-solubility in Opx in equilibrium with garnet that corrects for the effects

of late Fe-Mg exchange. Al concentrations in orthopyroxene are expected to be preserved from peak granulite conditions because of extremely slow diffusion of Al. In view of these arguments, we have applied the convergence method of Pattison et al. (2003) from the garnet-orthopyroxene-plagioclase-quartz assemblage, involving the following mineral equilibria: (1) almandine + 3 enstatite = pyrope + 3 ferrosilite; (2) almandine = 3 ferrosilite + Al-orthopyroxene; (3) almandine + grossularite + 3 quartz = 6 ferrosilite + 3 enstatite; (4) pyrope = 3 enstatite + Al-orthopyroxene; (5) 2 pyrope + grossularite + 3 quartz = 6 enstatite + 3 anorthite; and (6) grossularite + 2 Al-orthopyroxene + 3 quartz = 3 anorthite.

Among the six possible equilibria that can be written for the selected end-member phases, there are three independent equilibria shown in bold lines (Fig. 6). P-T plots of the unadjusted and adjusted core compositions of garnet/orthopyroxene along with the mineral equilibria are shown in this figure. The intersection of Fe-Mg exchange equilibrium 1 with the net-transfer equilibrium 3 represents the uncorrected Fe-Mg P-T estimate (Figs. 6A, 6C, and 6E). Intersection of equilibrium 2 with equilibrium 3 represents the uncorrected Fe-Al P-T estimate (Figs. 6A, 6C, and 6E). Equilibrium 2, based on Al solubility in orthopyroxene in the Fe-end member system, is a good method to retrieve peak temperatures because it is relatively robust to late exchange of Fe-Mg (Aranovich and Berman, 1997). Figures 6B, 6D, and and 6F show intersections of the mineral equilibria curves through adjustment of Fe-Mg ratios of garnet and orthopyroxene according to mass balance constraints, so that all equilibria intersect at a point referred as the corrected Fe-Mg-Al P-T estimate. The P-T estimated from the equilibria 1 to 6 for the UHT sapphirine-granulites from the Palni Hills is 1007°C, which is consistent with those derived from petrogenetic grid in the FMAS system (Raith et al., 1997). Using the same set of equilibria, core compositions for garnet orthopyroxene-bearing gneisses give intersection at 9.89 kbar and 937°C. Using the above equilibria, garnet-orthopyroxene core compositions for garnet-cordierite gneisses give a precise intersection at ca. 9.1 kbar and 914°C, thus lending support for the described UHT conditions.

Temperature and pressure values obtained from the intersection of mineral equilibria are computed in Table 3. No significant variation in peak P-T conditions is observed using different X_{Al} models. Model A and Model B provide maximum estimates

for X_{Al} Opx (see Fitzsimons and Harley, 1994; Aranovich and Berman, 1997). The temperature of metamorphism was probably buffered by solid-melt equilibria. For the post-peak exhumation history, the textures and mineral reactions preserved in these granulites are consistent with decompression followed by cooling (Mohan et al., 1996; Prakash, 1999; Prakash and Arima, 2003; Prakash et al., 2006b). The convergence method presented in this study indicates that granulites of the Palni Hills experienced maximum temperatures up to 1000°C (core), which is compatible with feldspar themometery discussed above.

Discussion and Conclusions

The data presented in this study further supports the prevalence of ultrahigh-temperature conditions in the Palni Hills. With the recent re-estimation of metamorphic condition based on the Al-orthopyroxene thermometer, there are clear indications that earlier P-T estimates (700–800°C and 5–7 kbar) underestimated the metamorphic conditions in this region. We believe that the proposed calculation procedure enables us to recover close-to-peak metamorphic conditions successfully. The re-integrated ternary feldspar compositions and retrieval calculations suggest UHT in the range of 900–1000°C at 9 kbar for the metamorphism of Palni Hills rocks. These high temperatures are consistent with the garnet-bearing mafic granulites observerd in Panrimalai (Palni Hills; Prakash et al., 2006a). This UHT metamorphism implies that the metapelites probably underwent extensive melting (Vielzeuf and Montel, 1994; Patino Douce and Beard, 1995). Prakash and Arima (2003) recorded evidence for melting and decompression reactions from the Palni Hills that are preserved in individual samples. The UHT assemblage opx-crd-sil-grt-kfs-qtz-spr and bt coexisted with melt in equilibrium at the thermal peak. These observations are confirmed by the present study.

UHT terrains distributed in Eurasia, Africa, Antarctica, North and South America, and Australia are shown in Figure 7. These UHT terrains lie within major Archean continental orogenic belts and Proterozoic shield areas. UHT granulites have been reported from a number of higher grade crustal segments around the world (Table 4). The tectonic setting required for the UHT metamorphism is still debated, and a great deal of current research revolves around this issue. Ultrahigh temperatures
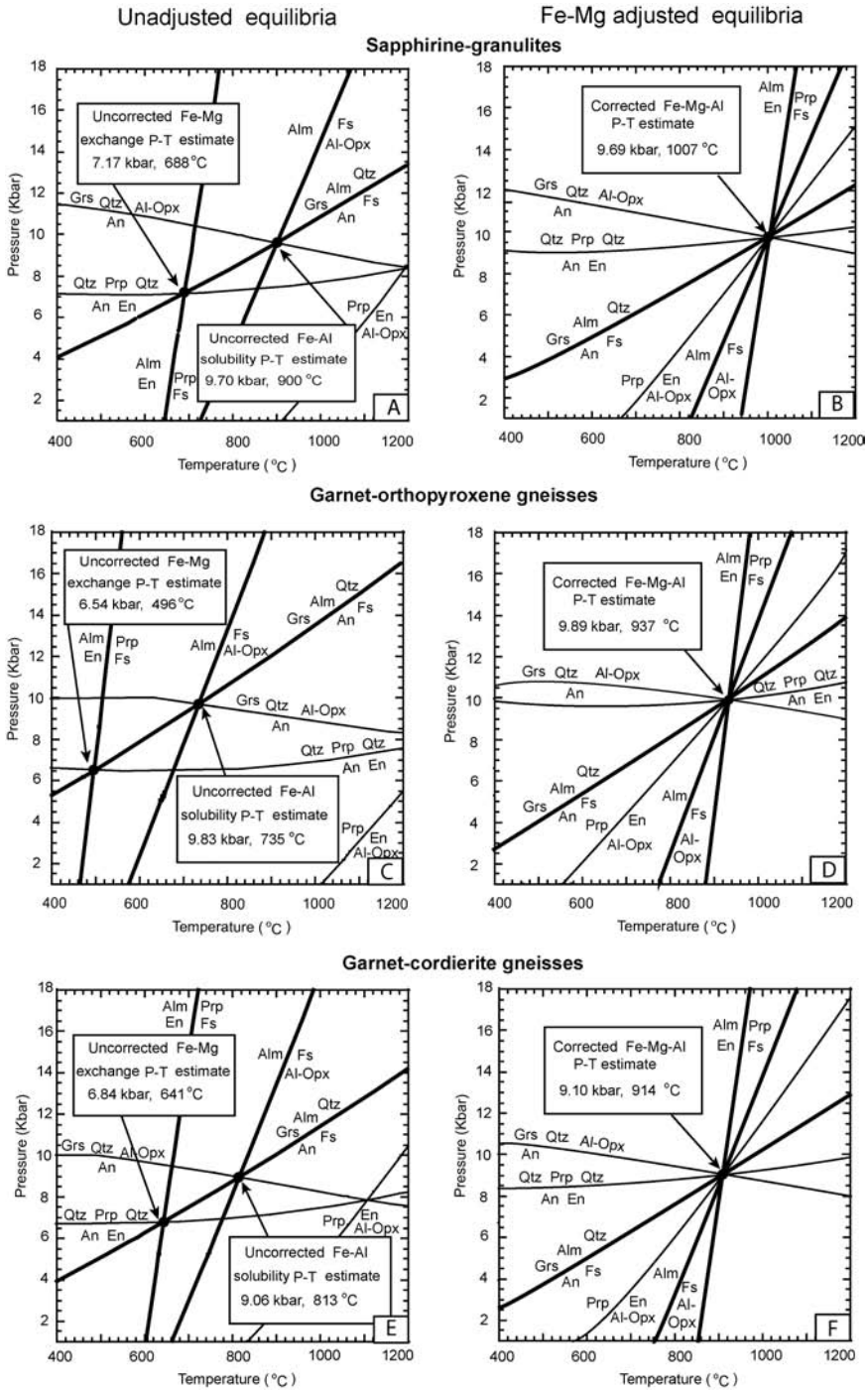
PRAKASH ET AL.

FIG. 6. P-T plots showing the convergence method of retrieval of the thermal peak conditions. A, C., and E display the typical spread in equilibria without adjustment of the mineral compositions. Of the six equilibria shown, only three are independent, and these are indicated in bold. B, D, and F show intersection of the curves of the mineral equilibria through adjustment of Fe-Mg ratios of garnet and orthopyroxene according to mass balance constraints so that all equilibria intersect at a point. See text for details.

TABLE 3. Grt-Opx-Pl-Qtz P-T Estimates Corrected for Late Fe-Mg Exchange

Rock type: Sapphirine-bearing granulites

I. Model A X_{Al}Opx (1-site Opx) = (Al/2) / 2

X_{Fe}Opx = Fe^{2+}/ 2 , X_{Mg}Opx = Mg / 2

Mode Grt = 10.00	ModeOpx = 10.00	Mode Bt = 10.00	Mode Crd = 10.00
X_{Fe}Grt = 0.502	X_{Mg}Grt = 0.449	X_{Mn}Grt = 0.012	X_{Ca}Grt = 0.037
X_{Fe}Opx = 0.266	X_{Mg}Opx = 0.614	X_{Al}Opx = 0.094	TotOpx = 0.974
X_{Fe}Bt = 0.239	X_{Mg}Bt = 0.650	X_{Al}Bt = 0.049	X_{Ti}Bt = 0.062
X_{Fe}Crd = 0.079	X_{Mg}Crd = 0.920	X_{Mn}Crd = 0.001	
X_{An}Pl = 0.461	X_{Ab}Pl = 0.508	X_{Or}Pl = 0.030	

Initial and converted P-T estimates and mineral compositions

	Converted (Final)	Initial	Difference
Fe Al GOPQ	1007°C 9.69 Kbar	900°C 9.70 Kbar	108°C –0.01 Kbar
GrtOpx GOPQ	1007°C 9.69 Kbar	688°C 7.17 Kbar	319°C 2.53 Kbar
GrtBt GOPQ	1007°C 9.69 Kbar	715°C 7.48 Kbar	292°C 2.22 Kbar
GrtCrd GOPQ	1007°C 9.69 Kbar	533°C 5.43 Kbar	475°C 4.27 Kbar
M/FM Grt	0.553	0.472	0.081
M/FM Opx	0.691	0.698	–0.007
M/FM Bt	0.699	0.731	–0.032
M/FM Crd	0.780	0.921	–0.140

II. Model B X_{Al}Opx (1-site Opx) = (Al/2) / sum

Where sum = Fe^{2+} + Mg + Mn + Ca + (Al/2). X_{Fe}Opx = Fe^{2+}/ sum

X_{Fe}Opx = 0.273	X_{Mg}Opx = 0.630	X_{Al}Opx = 0.097	TotOpx = 1.000

Initial and converted P-T estimates and mineral compositions

	Converted (final)	Initial	Difference
Fe Al GOPQ	1019°C 9.80 Kbar	906°C 9.51 Kbar	113°C 0.29 Kbar
GrtOpx GOPQ	1019°C 9.80 Kbar	684°C 6.90 Kbar	335°C 2.90 Kbar
GrtBt GOPQ	1019°C 9.80 Kbar	714°C 7.23 Kbar	306°C 2.57 Kbar
GrtCrd GOPQ	1019°C 9.80 Kbar	532°C 5.24 Kbar	487°C 4.56 Kbar
M/FM Grt	0.555	0.472	0.083
M/FM Opx	0.691	0.698	–0.007
M/FM Bt	0.698	0.731	–0.033
M/FM Crd	0.778	0.921	–0.143

TABLE 3. *Continued*

Rock type: Garnet-orthopyroxene bearing gneisses

I. Model A $X_{Al}Opx$ (1-site Opx) = (Al/2) / 2

$X_{Fe}Opx = Fe^{2+} / 2$, $X_{Mg}Opx = Mg / 2$

Mode Grt = 10.00	ModeOpx = 10.00	Mode Bt = 10.00	Mode Crd = 10.00
$X_{Fe}Grt = 0.517$	$X_{Mg}Grt = 0.409$	$X_{Mn}Grt = 0.024$	$X_{Ca}Grt = 0.050$
$X_{Fe}Opx = 0.228$	$X_{Mg}Opx = 0.691$	$X_{Al}Opx = 0.070$	TotOpx = 1.007
$X_{Fe}Bt = 0.190$	$X_{Mg}Bt = 0.667$	$X_{Al}Bt = 0.054$	$X_{Ti}Bt = 0.089$
$X_{Fe}Crd = 0.179$	$X_{Mg}Crd = 0.821$	$X_{Mn}Crd = 0.000$	
$X_{An}Pl = 0.451$	$X_{Ab}Pl = 0.524$	$X_{Or}Pl = 0.025$	

Initial and converted P-T estimates and mineral compositions

	Converted (final)	Initial	Difference
Fe Al GOPQ	937°C 9.89 Kbar	735°C 9.83 Kbar	202°C 0.07 Kbar
GrtOpx GOPQ	937°C 9.89 Kbar	496°C 6.54 Kbar	441°C 3.35 Kbar
GrtBt GOPQ	937°C 9.89 Kbar	516°C 6.80 Kbar	421°C 3.09 Kbar
GrtCrd GOPQ	937 oC 9.89 Kbar	751°C 10.06 Kbar	186°C –0.16 Kbar
M/FM Grt	0.553	0.442	0.111
M/FM Opx	0.707	0.752	–0.044
M/FM Bt	0.706	0.779	–0.073
M/FM Crd	0.805	0.821	–0.015

II. Model B $X_{Al}Opx$ (1-site Opx) = (Al/2) / sum

Where sum = Fe^{2+} + Mg + Mn + Ca + (Al/2). $X_{Fe}Opx = Fe^{2+}/$ sum

$X_{Fe}Opx = 0.228$	$X_{Mg}Opx = 0.691$	$X_{Al}Opx = 0.070$	TotOpx = 1.007

Initial and converted P-T estimates and mineral compositions

	Converted (final)	Initial	Difference
Fe Al GOPQ	940°C 9.92 Kbar	735°C 9.77 Kbar	205°C 0.15 Kbar
GrtOpx GOPQ	940°C 9.92 Kbar	495°C 6.48 Kbar	445°C 3.44 Kbar
GrtBt GOPQ	940°C 9.92 Kbar	515°C 6.76 Kbar	425°C 3.17 Kbar
GrtCrd GOPQ	940°C 9.92 Kbar	751°C 10.00 Kbar	189° C –0.07 Kbar
M/FM Grt	0.554	0.442	0.112
M/FM Opx	0.707	0.752	–0.044
M/FM Bt	0.705	0.779	–0.073
M/FM Crd	0.805	0.821	–0.016

TABLE 3. *Continued*

Rock type: Garnet-sillimanite ± cordierite gneisses

I. Model A $X_{Al}Opx$ (1-site Opx) = (Al/2) / 2

$X_{Fe}Opx = Fe^{2+}/2$, $X_{Mg}Opx = Mg / 2$

Mode Grt = 10.00	ModeOpx = 10.00	Mode Bt = 10.00	Mode Crd = 10.00
$X_{Fe}Grt = 0.529$	$X_{Mg}Grt = 0.407$	$X_{Mn}Grt = 0.019$	$X_{Ca}Grt = 0.044$
$X_{Fe}Opx = 0.285$	$X_{Mg}Opx = 0.633$	$X_{Al}Opx = 0.065$	TotOpx = 1.010
$X_{Fe}Bt = 0.255$	$X_{Mg}Bt = 0.626$	$X_{Al}Bt = 0.022$	$X_{Ti}Bt = 0.096$
$X_{Fe}Crd = 0.182$	$X_{Mg}Crd = 0.816$	$X_{Mn}Crd = 0.001$	
$X_{An}Pl = 0.416$	$X_{Ab}Pl = 0.572$	$X_{Or}Pl = 0.011$	

Initial and converted P-T estimates and mineral compositions

	Converted (final)	Initial	Difference
Fe Al GOPQ	914°C 9.10 Kbar	813°C 9.06 Kbar	101°C 0.05 Kbar
GrtOpx GOPQ	914°C 9.10 Kbar	641°C 6.84 Kbar	273°C 2.26 Kbar
GrtBt GOPQ	914°C 9.10 Kbar	659°C 7.06 Kbar	256°C 2.04Kbar
GrtCrd GOPQ	914°C 9.10 Kbar	748°C 8.20 Kbar	166°C 0.90 Kbar
M/FM Grt	0.500	0.435	0.066
M/FM Opx	0.669	0.690	−0.021
M/FM Bt	0.671	0.711	−0.040
M/FM Crd	0.783	0.817	−0.034

II. Model B $X_{Al}Opx$ (1-site Opx) = (Al/2) / sum

Where sum = $Fe^{2+} + Mg + Mn + Ca + (Al/2)$. $X_{Fe}Opx = Fe^{2+}/$ sum

$X_{Fe}Opx = 0.288$	$X_{Mg}Opx = 0.641$	$X_{Al}Opx = 0.066$	TotOpx = 1.021

Initial and converted P-T estimates and mineral compositions

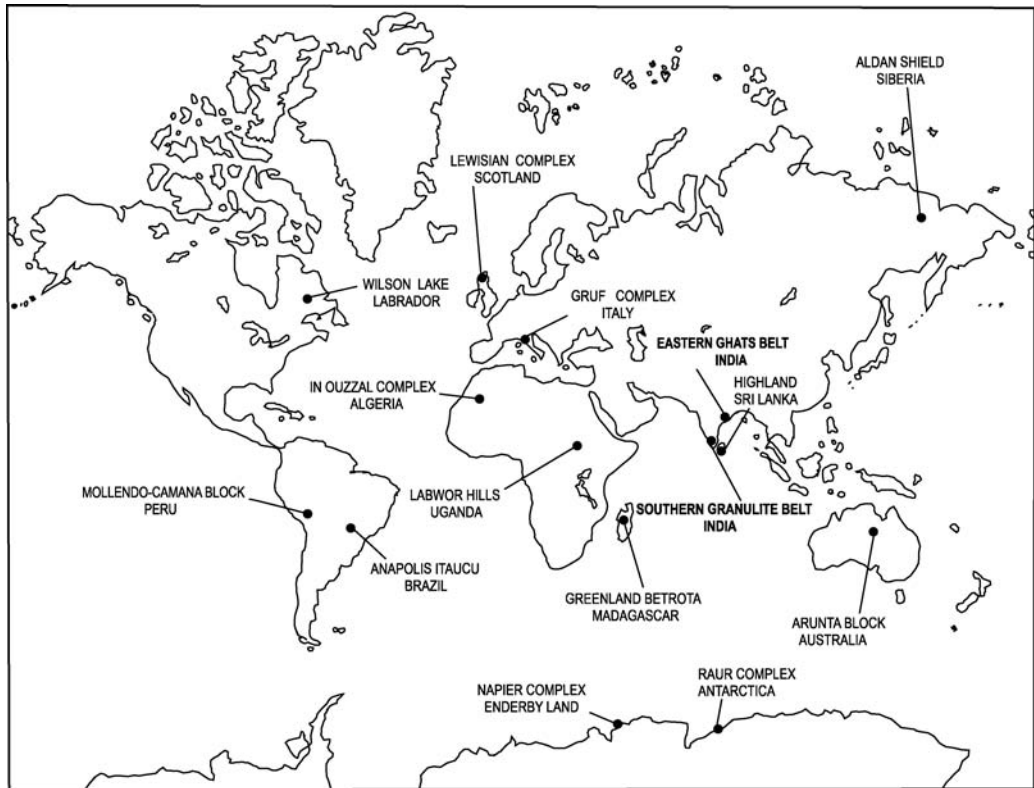|	Converted (final)	Initial	Difference
Fe Al GOPQ	919°C 9.15 Kbar	814°C 8.97 Kbar	104°C 0.18 Kbar
GrtOpx GOPQ	919°C 9.15Kbar	640°C 6.73 Kbar	279°C 2.41 Kbar
GrtBt GOPQ	919°C 9.15 Kbar	658°C 6.96 Kbar	261°C 2.19 Kbar
GrtCrd GOPQ	919°C 9.15 Kbar	748°C 8.10 Kbar	117°C 1.04 Kbar
M/FM Grt	0.501	0.435	0.067
M/FM Opx	0.669	0.690	−0.022
M/FM Bt	0.670	0.711	−0.040
M/FM Crd	0.782	0.817	−0.036

FIG. 7. Global distribution of UHT regionally metamorphosed terrains.

signify anomalously high thermal input, which is of fundamental importance in understanding the P-T structure and related petrological processes of the lower crust. Speculations regarding the cause of the high thermal input range from influx of mantle-derived, hot CO_2-rich fluids (Newton et al., 1980) to radioactive heating (with or without magmatic input) in an overthickened continental crust (Thompson and England, 1984; Hodges, 1991; Huerta et al., 1999), magmatic under/intraplating (Bohlen, 1987) to lithospheric/crustal thinning with or without magmatic input (Oxburgh, 1990). Each individual area requires careful study to test the applicability of these models, inasmuch as many new concepts are offered for ultrahigh-temperature metamorphism (Harley, 2004). Although it has long been established that what drives metamorphism and metamorphic processes is heat, the thermal source remains enigmatic (Jamieson et al., 1998). The distribution and transport of heat through

crustal rocks have not been ascertained in much detail (Treloar and O'Brien, 1998). Identifying the source of adequate heat to achieve the peak temperatures that is required by UHT metamorphism has been the real concern for metamorphic petrologists. It is now generally accepted that regional granulite-facies metamorphism requires an input of extra heat over and above that which is available from a thickened crust (Ashwal et al., 1991). P-T-t paths recovered from high-grade granulites are controlled by: (a) thermal perturbation and (b) relaxation of thermal perturbation toward a steady state. In order to produce temperatures in excess of 900°C, syn-post accretion of mantle-derived magma is necessary to enhance the total heat buget. Models of magmatic underplating in crust of normal thickness involving the dominance of mafic magmatic intrusives in the lowermost crust would also produce elevated geotherms. Moreover, dehydration melting experiments on hydrous silicates require an extra heat input, and

TABLE 4. UHT Terrains in the World

UHT terrains	UHT rock types	Reference(s)
Southern granulite belt, India	Sapphirine-granulites	Raith et al.,1997
	Marble	Satish Kumar, 2000
	Garnet-granulites	Nandakumar and Harley, 2000
	Sapphirine-granulites	Prakash and Arima, 2003
	Sapphirine-granulites	Sajeev et al.,2004
	Mafic granulites	Prakash et al., 2006a
Eastern Ghats belt, India	Spinel-granulites	Dasgupta et al., 1995
	Sapphirine-granulites	Mohan et al., 1997
	Sapphirine-granulites	Sarkar et al., 2003
	Garnet-granulites	Santosh et al., 2004
Napier Complex, Antarctica	Sapphirine-granulites	Harley and Motoyoshi, 2000
	Garnet-granulites	Hokada, 2001
	Sapphirine-granulites	Tsunogae et al., 2002
	Sapphirine-granulites	Hokada et al., 2004
	Sapphirine-granulites	Hokada and Harley, 2004
Raur Group, East Antarctica	Garnet-Opx-Sill gneisses	Harley,1998b
Ouzzal Complex, Algeria	Corundum-granulites	Ouzegane et al., 2003
Andriamena, Madagascar	Magnesian-granulites	Paquette et al., 2004
Mollendo-Camana, Peruvian Andes	Aluminous-gneisses	Martingole and Martelat, 2003
Anápolis-Itauçu Complex, Brazil	Sapphirine-granulites	Moraes et al., 2002
Rogaland, Norway	Granitic gneisses	Moller et al., 2002
Saxon Massif, Germany	Sapphirine-granulites	Rotzler and Romer, 2001
Schwarzwald, Germany	Garnet-granulites	Marschall et al., 2003
Epupa Complex, Namibia	Garnet-Opx granulites	Brandt et al., 2003
Highland Complex, Sri Lanka	Sapphirine-granulites	Sajeev and Osanai, 2004
	Garnet-granulites	Santosh et al., 2004
Kontum Massif, Vietnam	Garnet-Opx-Sill-Crd gneisses	Osanai et al., 2004
Lewisian Complex, Scotland	Sapphirine-granulites	Baba, 2003,2004

dehydration melting plays a vital role during the formation of granulites whose P-T evolution lies above the wet solidus for crustal rocks (Dooley and Patino Douce, 1996).

Acknowledgments

Peter Raase for providing the feldspar thermometer programs and T. Saito for discussions and comments on this work. Anonymous reviewers are thanked for their constructive comments.

REFERENCES

Aranovich, L. Ya., and Berman, R. G., 1997, A new garnet-orthopyroxene thermometer based on the reversed Al_2O_3 solubility in $FeO-Al_2O_3-SiO_2$ orthopyroxene: American Mineralogist, v. 82, p. 345–353.

Ashwal, L. D., Moran, P., and Hoisch, T. D., 1991, Tectonics and heat sources for granulite metamorphism of supracrustal-bearing terrains: Precambrian Research, v. 55, p. 525–538.

Baba, S. 2003, Two stages of sapphirine formation during prograde and retrograde metamorphism in the palaeoproterozoic Lewisian Complex in South Harris, NW Scotland: Journal of Petrology, v.44, p. 329–354.

Baba, S. 2004, Palaeoproterozoic UHT metamorphism in the Lewisian complex and North region: Journal of Mineralogical and Petrological Sciences, v. 99, p. 202–212.

Bohlen, S. R. 1987, Pressure-temperature-time paths and a tectonic model for the evolution of granulites: Journal of Geology, v. 95, p. 617–632.

Brandt, S., Klemd, R., and Okrusch, M., 2003, Ultrahigh-temperature metamorphism and multistage evolution of garnet-orthopyroxene granulites from the Proterozoic Epupa Complex, NW Namibia: Journal of Petrology, v. 44, p. 1121–1144.

Braun, S. R., Raith, M., and Ravindra Kumar, G. R., 1996, Dehydration-melting phenomena in leptynitic gneisses and the generation of leucogranites: A case study from the Kerala Khondalite belt, southern India: Journal of Petrology, v. 37, p. 1285–1305.

Chacko, T., Lamb, M., and Farquhar, J., 1996, Ultra-high temperature metamorphism in the Kerala Khondalite belt, *in* Santosh, M., and Yoshida, M., eds., The Archaean and Proterozoic terrains in southern India within east Gondwana: Gondwana Research Group Memoir, v. 3, p. 157–165.

Das, K., Fujino, K., Tomioka, N., and Miura, H., 2005, Experimental data on Fe and Mg partitioning between coexisting sapphirine and spinel: An empirical geothermometer and its application: European Journal of Mineralogy, v. 18, p. 49–58.

Dasgupta, S., Sengupta, P., Ehl, J., Raith, M., and Bardhan, S., 1995, Reaction textures in a suite of spinel granulites from the Eastern Ghats Belt, India: Evidence for polymetamorphism, a partial petrogenetic grid in the system KFMASH and the role of ZnO and Fe_2O_3: Journal of Petrology, v. 36, p. 435–461.

Dooley, D. F., and Patino Douce, A. E., 1996, Fluid-absent melting of F-rich phlogopite + rutile + quartz: American Mineralogist, v. 81, p. 202–212.

Elkins, L. T., and Grove, T. L., 1990, Ternary feldspar experiments and thermodynamic models: American Mineralogist, v. 75, p. 544–559.

Fitzsimons, I. C. W., and Harley, S. L., 1994, The influence of retrograde cation exchange on P-T estimates of granulite and a convergence technique for the recovery of peak metamorphic conditions: Journal of Petrology, v. 35, p. 543–576.

Frost, B. R., and Chacko, T., 1989, The granulite uncertainty principle: Limitations on thermobarometry in granulites: Journal of Geology, v. 97, p. 435–450.

Fuhrman, M. L., and Lindsley, D. H., 1988, Ternary-feldspar modeling and thermometry: American Mineralogist, v. 73, p. 201–215.

Grove, T. L., Barker, M. B., and Kinzler, R. J., 1984, Coupled CaAl-NaSi diffusion in plagioclase feldspar: Experiments and applications to cooling rate speedometery: Geochimica et Cosmochimica Acta, v. 48, p. 2113–2121.

Harley, S. L., 1989, The origins of granulites: A metamorphic perspective: Geological Magazine, v. 126, p. 215–247.

Harley, S. L., 1998a, On the occurrence and characterisation of ultrahigh-temperature crustal metamorphism, *in* Treloar, P. J., and O'Brien, P., eds., What drives metamorphism and metamorphic reactions?: Geological Society of London, Special Publications, v. 138, p. 81–107.

Harley, S. L. 1998b, Ultrahigh temperature granulite metamorphism (1050°C, 12 kbar) and decompression in garnet (Mg70) orthopyroxene sillimanite gneisses from the Rauer Group, East Antarctica: Journal of Metamorphic Geology, v. 16, p. 541–562.

Harley, S. L., 2004, Extending our understanding of ultrahigh temperature crustal metamorphism: Journal of Mineralogical and Petrological Sciences, v. 99, p. 140–158.

Harley, S. L., and Motoyoshi, Y., 2000, Al zoning in orthopyroxene in a sapphirine quartzite: Evidence for > 1120°C UHT metamorphism in Napier complex, Antarctica, and implications for the entropy of sapphirine: Contributions to Mineralogy and Petrology, v. 138, p. 293–307.

Harris, N. B. W., Holt, R. W., and Drury, S. A., 1994, Crustal evolution in South India: Constraints from Nd isotopes: Journal of Geology, v. 102, p. 139–150.

Hayob, J. L., Essene, E. J., Ruiz, J., Ortega-Gutierrez, F., and Aranda-Gomez, J. J., 1989, Young high-temperature granulites from the base of the crust in central Mexico: Nature, v. 342, p. 265–268.

Hodges, K. V., 1991, Pressure-temperature-time paths: Annual Review of Earth and Planetary Sciences, v. 19, p. 207–236

Hokada, T., 2001, Felspar thermometry in ultrahigh-temperature metamorphic rocks: Evidence of crustal metamorphism attaining ~1100°C in the Archean

Napier complex, East Antarctica: American Mineralogist, v. 86, p. 932–938.

Hokada, T., and Harley, S. L., 2004, Zircon growth in UHT leucosome: Constraints from zircon-garnet rare earth elements (REE) relations in Napier complex, East Antarctica: Journal of Mineralogical and Petrological Sciences, v. 99, p. 180–190.

Hokada, T., Misawa, K., Yokoyama, K., Shiraishi, K., and Yamaguchi, A., 2004, SHRIMP and electron microprobe chronology of UHT metamorphism in the Napier Complex, East Antarctica: Implications for zircon growth at >1,000°C: Contributions to Mineralogy and Petrology, v. 147, p. 1–20.

Huerta, A. D., Royden, L. H., and Hodges, K. V., 1999, The effects of accretion, erosion, and radiogenic heat on the metamorphic evolution of collisional orogens: Journal of Metamorphic Geology, v. 17, p. 349–366.

Jamieson, R. A., Beaumont, C., Fullsack, P., and Lee, B., 1998, Barrovian regional metamorphism: Where's the heat?, *in* Treloar, P. J., and O'Brien, P., eds., What drives metamorphism and metamorphic reactions?: Geological Society of London, Special Publications, v. 138, p. 23–51.

Koshimoto, S., Tsunogae, T., and Santosh, M., 2004, Sapphirine and corundum bearing ultrahigh temperature rocks from the Palghat-Cauvery shear system, Southern India: Journal of Mineralogical and Petrological Sciences, v. 99, p. 298–310.

Kroll, H., Evangelakakis, C., and Voll, G., 1993, Two-feldspar geothermometery: A review and revision for slowly cooled rocks: Contributions to Mineralogy and Petrology, v. 114, p. 510–518.

Lindsley, D. H., and Nekvasil, H., 1989, A ternary feldspar model for all reasons: EOS (Transactions of the American Geophysical Union), v. 70, p. 506.

Liu, M., and Yund, R. A., 1992, NaSi-CaAl interdiffusion in plagioclase: American Mineralogist, v. 77, p. 275–283.

Marschall, H. R., Kalt, A., and Hanel, M., 2003, P-T evolution of a Variscan lower-crustal segment: A study of granulites from the Schwarzwald, Germany: Journal of Petrology, v. 44, p. 227–253.

Martignole, J., and Martelat, J. E., 2003, Regional-scale Grenvillian-age UHT metamorphism in the Mollendo-Camana Block (basement of the Peruvian Andes): Journal of Metamorphic Geology, v. 21, p. 99–120.

Mohan, A., Prakash, D., and Motoyoshi, Y., 1996, Decompressional P-T history in the sapphirine-bearing granulites from Kodaikanal, southern India: Journal of South East Asian Earth Sciences. v. 14, p. 231–243.

Mohan, A., Sharma, I. N., and Singh, P. K., 2005, UHT metamorphism and continental orogenic belts, *in* Thomas, H., ed., Metamorphism and crustal evolution: New Delhi, India: Atlantic Publishers, p. 314–335.

Mohan, A.,Tripathi, P., and Motoyoshi, Y., 1997, Reaction history of sapphirine granulites and decompressional

P-T path in a granulite complex from Eastern Ghats: Proceedings of the Indian Academy of Sciences (Earth and Planetary Sciences), v. 106, p. 115–129.

Moller, A., O'Brien, P. J., Kennedy, A., and Kroner, A., 2002, Polyphase zircon in ultrahigh-temperature granulites (Rogaland, SW Norway): Constraints for Pb diffusion in zircon: Journal of Metamorphic Geology, v. 20, p. 727–740.

Moraes, R., Brown, M., Fuck, R. A., Camargo, M. A., and Lima, T. M., 2002, Characterization and P-T evolution of melt-bearing ultrahigh-temperature granulites: An example from the Anapolis-Itaucu Complex of the Brasilia Fold Belt, Brazil: Journal of Petrology, v. 43, p. 1673–1705.

Nandakumar, V., and Harley, S. L. 2000, A reappraisal of the pressure-temperature path of granulites from the Kerala Khondalite belt, southern India: Journal of Geology, v. 108, p. 687–703.

Newton, R. C., Smith, J. V., and Windley, B. F. 1980, Carbonic metamorphism, granulites, and crustal growth: Nature, v. 288, p. 45–50.

Osanai, Y., Nakano, N., Owada, M., Nam, T. N., Toyoshima, T., Tsunogae, T., and Binh, P., 2004, Permo-Triassic ultrahigh-temperature metamorphism in the Kontum massif, central Vietnam: Journal of Mineralogical and Petrological Sciences, v. 99, p. 225–241.

Ouzegane, K., Guiraud, M., and Kienast, J. R., 2003, Prograde and retrograde evolution in high-temperature corundum granulites (FMAS and FMASh systems) in Ouzzal terrain (NW Hoggar, Algeria): Journal of Petrology, v. 44, p. 517–545.

Oxburgh, E. R., 1990, Some thermal aspects of granulite history, *in* Vielzeuf, D., and Vidal, Ph., eds., Granulites and crustal evolution: NATO ASI Series, v. 311, p. 569–580.

Paquette, J. L., Goncalves, P., Devouard, B., and Nicollet, C., 2004, Micro-drilling ID-TIMS U-Pb dating of single monazites: A new method to unravel complex poly-metamorphic evolutions. Application to the UHT granulites of Andriamena (North-Central Madagascar): Contributions to Mineralogy and Petrology, v. 147, p. 110–122.

Patino Douce, A. E., and Beard, J. S., 1995, Dehydration-melting of biotite gneiss and quartz amphibolite from 3 to 15 kbar: Journal of Petrology, v. 37, p. 999–1024.

Pattison, D. R. M., and Begin, N. J., 1994, Hierachy of closure temperatures in granulites and the importance of an intergranular exchange medium (melt?) in controlling maximum Fe-Mg exchange temperatures: Mineralogical Magazine, v. 58A, p. 694–695.

Pattison, D. R. M., Chacko, T., Farquhar, J., and McFarlane, C. R. M., 2003, Temperatures of granulite-facies metamorphism: Constraints from experimental phase equilibria and thermobarometry corrected for

retrograde exchange: Journal of Petrology, v. 44, p. 867–900.

Prakash, D., 1999, Cordierite-bearing gneisses from Kodaikanal, South India: Textural relationship and P-T conditions: The Journal of Geological Society of India, v. 54, p. 347–358.

Prakash, D., and Arima, M., 2003, High-temperature dehydration melting and decompressive textures in Mg-Al granulites from the Palni Hills, South India: Polar Geosciences, v. 16, p. 149–175.

Prakash, D., Arima, M., and Mohan, A., 2006a, Ultra-high-temperature mafic granulites from Panrimalai, South India: Constraints from phase equilibria and thermobarometry: Journal of Asian Earth Sciences, in press.

Prakash, D., Arima, M., and Mohan, A., 2006b, Colour-coded compositional mapping of orthopyroxene-plagioclase symplectites in mafic granulites from Panrimalai, South India: The Journal of Geological Society of India, in press.

Raase, P., 1998, Feldspar thermometry: A valuable tool for deciphering the thermal history of granulite-facies rocks, as illustrated with metapelites from Sri Lanka: The Canadian Mineralogist, v. 36, p. 67–86.

Raith, M., Karmakar, S., and Brown, M., 1997, Ultra-high-temperature metamorphism and multi-stage decompressional evolution of sapphirine granulites from the Palni Hill ranges, Southern India: Journal of Metamorphic Geology, v. 36, p. 891–931.

Rotzler, J., and Romer, R. L., 2001, P-T-t evolution of ultra-high-temperature granulites from the Saxon granulite massif, Germany. Part I: Petrology: Journal of Petrology, v. 42, p. 1995–2013.

Sajeev, K., and Osanai, Y., 2004, Ultrahigh-temperature metamorphism (1150°C, 12 kbar) and multistage evolution of Mg-, Al-rich granulites from the Central Highland Complex, Sri Lanka: Journal of Petrology, v. 45, p. 1821–1844.

Sajeev, K., Osanai, Y., and Santosh, M., 2004, Ultra-high-temperature metamorphism followed by two-stage decompression of garnet orthopyroxene silli-manite granulites from Ganguvarpatti, Madurai block, southern India: Contribution to Mineralogy and Petrology, v. 148, p. 29–46.

Santosh, M., Tsunogae, T., and Yoshikura, S., 2004, "Ultrahigh density" carbonic fluids in ultrahigh-temperature crustal metamorphism: Journal of Mineralogical and Petrological Sciences, v. 99, p. 164–179.

Sarkar, S., Santosh, M., Dasgupta, S., and Fukuoka, M., 2003, Very high density CO_2 associated with ultra-high-temperature metamorphism in the Eastern Ghats granulite belt, India: Geology, v. 31, p. 51–54.

Satish Kumar, M., 2000, Ultrahigh-temperature metamorphism in Madurai granulites, southern India: Evidence from carbon isotope thermometry: Journal of Geology, v. 108, p. 479–486.

Sriramguru, K., Janardhan, A. S., Basava, S., and Basava-lingu, B., 2002, Prismatine- and sapphirine-bearing assemblages from Rajapalaiyam area, Tamil Nadu: Origin and metamorphic history: The Journal of the Geological Society of India, v. 59, p. 103–112.

Tamashiro, T., Santosh, M., Sajeev, K, Morimoto, T., and Tsunogae, T., 2004, Multistage orthopyroxene formation in ultrahigh-temperature granulites of Ganguvar-patti, southern India: Implications for complex metamorphic evolution during Gondwana assembly: Journal of Mineralogical and Petrological Sciences, v. 99, p. 279–297.

Tateishi, K., Tsunogae, T., Santosh, M., and Janardhan, A. S., 2004, First report of sapphirine + quartz assem-blage from southern India: Implications for ultra-high-temperature metamorphism: Gondwana Research, v. 7, p. 899–912.

Thompson, A. B., and England, P. C., 1984, Pressure-tem-perature-time paths of regional metamorphism II: Their inference and interpretation using mineral assemblages in metamorphic rocks: Journal of Petrol-ogy, v. 25, p. 929–954.

Treloar, P. J., and O'Brien, P. J., 1998, Introduction, *in* Treloar, P. J., and O'Brien, P. J., eds., What drives metamorphism and metamorphic reactions?: Geologi-cal Society of London, Special Publications, v. 138, p. 1–5.

Tsunogae, T., and Santosh, M., 2003, Sapphirine and corundum-bearing granulites from Karur, Madurai block, Southern India: Gondwana Research, v. 6, p. 925–930.

Tsunogae, T., Santosh, M., Osanai, Y., Owada, M., Toyo-shima, T., and Hakada, T., 2002, Very high-den-sity carbonic fluid inclusions in sapphirine-bearing granulites from Tonagh Island in the Archean Napier Complex, East Antarctica: Implications for CO_2 infil-tration during ultrahigh-temperature (T>1100°C) metamorphism: Contributions to Mineralogy and Petrology, v. 143, p. 279–299.

Vielzeuf, D., and Montel, J. M., 1994, Partial melting of metagreywackes. Part I. Fluid-absent experiments and phase relationships: Contributions to Mineralogy and Petrology, v. 117, p. 375–393.

Yoshimura, Y., Motoyoshi, Y., Grew, E. S., Miyamoto, T., Carson, C. J., and Dunkley, D. J., 2000, Ultrahigh-tem-perature metamorphic rocks from Howard hills in the Napier complex, East Antarctica: Polar Geosciences, v. 13, p. 60–85.

Yund, R. A., 1986, Interdiffusion of NaSi-CaAl in peris-terite: Physics and Chemistry of Minerals, v. 13, p. 11–16.